# *INVESTIGATION OF THE PHOTOEFFECT IN LIGHT NUCLEI*

A. N. GORBUNOV, V. A. DUBROVINA, V. A. OSIPOVA, V. S. SILAEVA, and P. A. CERENKOV

Submitted to JETP editor October 28, 1961

J. Exptl. Theoret. Phys. (U.S.S.R.) **42**, 747-757 (March, 1962)

A cloud chamber was used to measure the absolute yields of the different photonuclear reactions in nitrogen, oxygen, and neon and also the quantities $\sigma_0$, $\sigma_{-1}$, and $\sigma_{-2}$. The experimental values of these quantities are compared with theoretical values obtained from E1 absorption sum rules. The mean square radii of the charge distributions are obtained for $N^{14}$, $O^{16}$, and $Ne^{20}$.

## 1. INTRODUCTION

THE theoretical treatment of the effective cross sections of the photonuclear effect on the basis of different models is fraught with great difficulties because the nuclear wave function of the ground state and even more so of the excited states are not well known. Up to now such calculations have been performed [1-4] only for the doubly "magic" nuclei $O^{16}$, $Ca^{40}$, and $Pb^{208}$, which have only a relatively small number of possible E1 transitions. For other nuclei the calculations become too involved because of the large number of participating transitions.

It is known (see, e.g., [5]) that these difficulties can be frequently avoided by summing over all excited states and using sum rules that allow the determinations of integrals of the type

$$\sigma_0 = \int \sigma(E)\, dE, \qquad \sigma_{-1} = \int \sigma(E)\, E^{-1} dE, \qquad \sigma_{-2} = \int \sigma(E)\, E^{-2} dE \qquad (1)$$

etc, where $\sigma(E)$ is the total nuclear photon absorption cross section or the cross section for transitions with a given multipolarity. Here the results depend only on the assumptions concerning the ground-state wave function.

Since the sum rules allow the determination of the basic characteristics of the photonuclear cross section (the integrated E1 absorption cross section; the position of the giant resonance peak $E_{max} \approx \sigma_0/\sigma_{-1}$), they can serve as an important check on results obtained from specific models. Up to now the experimental data on the quantities $\sigma_0$, $\sigma_{-1}$, $\sigma_{-2}$ etc, which can be obtained from sum rules, are incomplete. For a number of heavy nuclei these quantities have been measured only up to excitation energies of $\sim 25$ MeV. For the light nuclei the data for $\sigma_0$, $\sigma_{-1}$, and $\sigma_{-2}$ have been obtained only for deuterium and helium.

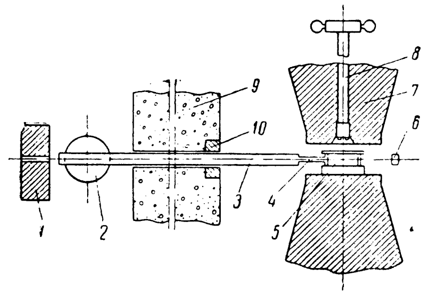


FIG. 1. Diagram of the experimental apparatus: 1—collimator, 2—cleaning magnet, 3—vacuum tube, 4—beam entrance, 5—cloud chamber, 6—ionization chamber, 7—magnet, 8—photo camera, 9—concrete wall, 10—lead shield.

In connection with the theoretical importance of the sum rules, it was thought worth while to obtain experimental data on the quantities $\sigma_0$, $\sigma_{-1}$, and $\sigma_{-2}$ for a number of light nuclei. In the present paper we give the results* of the measurement of these quantities for the nuclei of nitrogen, oxygen, and neon which have been obtained in a cloud chamber with bremsstrahlung of maximum energy $E_{\gamma max} = 170$ MeV.

## 2. EXPERIMENTAL METHOD

The experimental setup is shown schematically in Fig. 1. The bremsstrahlung beam is collimated in the lead collimator 1 (slit width either $3 \times 8$ mm or $4 \times 12$ mm) and enters through a thin aluminum window into the vacuum tube 3. The electrons and positrons originating in the collimator and the window are deflected by the cleaning magnet 2 and are absorbed in the concrete wall 9 and the lead absorber 10. Then the beam enters the working region of the cloud chamber 5 through a window 4 consisting of a triacetate cellulose film 70 $\mu$ thick. The cloud chamber had a diameter of

*Preliminary results have been communicated at the Tashkent Conference on Peaceful Uses of Atomic Energy, 1959[6].

**Table I**

| Reaction | Reaction Threshold, MeV | | | Reaction | Reaction Threshold, MeV | | |
|---|---|---|---|---|---|---|---|
| | N | O | Ne | | N | O | Ne |
| $(\gamma, n)$ | 10.54 | 15.60 | 16.79 | $(\gamma, 2\alpha)$ | 16.06 | — | 11.82 |
| $(\gamma, p)$ | 7.54 | 12.11 | 12.79 | $(\gamma, p\alpha n)$ | 19.86 | 34.56 | 27.61 |
| $(\gamma, d)$ | 10.26 | 20.72 | 20.99 | $(\gamma, 2pn)$ | 28.44 | 30.48 | 28.81 |
| $(\gamma, \alpha)$ | 11.61 | 7.15 | 4.67 | $(\gamma, 2\alpha n)$ | — | — | 30.53 |
| $(\gamma, pn)$ | 12.49 | 22.94 | 23.22 | $(\gamma, 4\alpha)$ | — | 14.43 | |
| $(\gamma, \alpha n)$ | 20.05 | 25.86 | 20.26 | $(\gamma, 3\alpha pn)$ | 19.77 | — | |
| $(\gamma, p\alpha)$ | 18.20 | 23.10 | 16.78 | $(\gamma, 2p2n3\alpha)$ | — | 42.71 | |
| $(\gamma, 2p)$ | 25.08 | 22.32 | 20.76 | | | | |

30 cm and a height of 8 cm and was filled with the gas under investigation.

In the experiments with nitrogen and oxygen the cloud chamber was filled to 326 and 265 mm Hg (at 15°C) respectively. In the neon runs the chamber was filled with a 50% neon and 50% hydrogen mixture to ~ 1000 mm Hg. During the experiments the relative values of the stopping power of nitrogen, oxygen, and neon after expansion were 0.39, 0.29, and 0.50 respectively. At such stopping powers the track length of the recoiling nuclei from $(\gamma, p)$, $(\gamma, n)$, and $(\gamma, pn)$ reactions were of the order of a few millimeters and were not strongly scattered.

The cloud chamber was operated in a 10.5 kOe magnetic field. The expansion of the chamber was timed such [7] that the photon beam pulse arrived after the expansion. This resulted in a considerable decrease in the distortion of the tracks which could occur due to the motion of the gas during the expansion. The repetition cycle was about 30—40 seconds. Between the chamber expansions the synchrotron continued to work at its normal rate of 50 pulses per second, so that the electronic circuitry could be used.

The intensity of the photon pulses which were used to irradiate the cloud chamber were measured by means of a pulsed ionization chamber. It had been calibrated in terms of the absolute $\beta^+$ activity associated with the reaction $C^{12}(\gamma, n)C^{11}$ the yield of which has been carefully measured by Barber et al. [8]

### 3. IDENTIFICATION OF THE PHOTONUCLEAR REACTIONS

The photonuclear reactions observed in the irradiation of nitrogen, oxygen, and neon in the cloud chamber with bremsstrahlung of maximum energy 170 MeV are listed in Table I.

In addition, a small number of stars with 3 to 6 prongs were also observed. However, their identification was difficult.

The reaction $(\gamma, n)$ [or $(\gamma, 2n)$] is characterized by a single dense track of the recoil nucleus, 15—20 mm long. In the scanning we attributed all single tracks of this type to the reaction $(\gamma, n)$, since according to O'Connell et al [9] the ratio of the integrated cross sections of the reactions $(\gamma, 2n)$ and $(\gamma, n)$ in light elements with $A = 4n$ is of the order of a few tenths of one per cent.

In the reactions $(\gamma, p)$, $(\gamma, d)$, and $(\gamma, \alpha)$ the final state contains only two particles, which are thus emitted in opposite directions in the center-of-mass system. In the laboratory system the angle between the tracks is also close to 180° and it opens away from the direction of the incoming beam. Furthermore, the tracks and the photon beam are coplanar. Since the final state in the reactions $(\gamma, pn)$ and $(\gamma, \alpha n)$ contains three particles, the outgoing charged particles are emitted at arbitrary angles with respect to each other and the photon beam. This way they can be easily distinguished from the reactions $(\gamma, p)$ and $(\gamma, \alpha)$. The reactions $(\gamma, p)$ and $(\gamma, pn)$ can be easily distinguished from the reactions $(\gamma, \alpha)$ and $(\gamma, \alpha n)$, owing to the different track density of the protons and $\alpha$-particles.

The reactions $(\gamma, p)$ and $(\gamma, d)$ cannot be distinguished visually. Therefore we have assumed all reactions of the "type $(\gamma, p)$" as due to the reaction $(\gamma, p)$, remembering that owing to isospin selection rules the cross section for $(\gamma, d)$ reactions must be two orders of magnitude smaller than the $(\gamma, p)$ cross section. Such a yield ratio of the reactions $(\gamma, p)$ and $(\gamma, d)$ has indeed been observed [10] in the photodisintegration of helium.

The reactions $(\gamma, p\alpha)$ and $(\gamma, p\alpha n)$; $(\gamma, 2p)$ and $(\gamma, 2pn)$; $(\gamma, 2\alpha)$ and $(\gamma, 2\alpha n)$ were distinguished qualitatively by means of considerations following from momentum conservation and track densities.

In order to exclude the possibility of omissions of photonuclear events or of errors in their identification the cloud chamber pictures were scanned by means of stereo magnifying glasses twice by

**Table II**

| Reaction type | Number of observed events | | | | Yield relative to the $(\gamma, p)$ yield | | | |
|---|---|---|---|---|---|---|---|---|
| | $He^4$ | $N^{14}$ | $O^{16}$ | Ne | $He^4$ | $N^{14}$ | $O^{16}$ | Ne |
| $(\gamma, p)$ | 2835 | 1277 | 2610 | 2184 | 1 | 1 | 1 | 1 |
| $(\gamma, n)$ | 2685 | 708 | 1560 | 1112 | 0.95 | 0.55 | 0.60 | 0.51 |
| $(\gamma, pn)$ | 484 | 2420 | 561 | 428 | 0.17 | 1.90 | 0.22 | 0.20 |
| $(\gamma, \alpha)$ | — | 160 | 154 | 242 | — | 0.12 | 0.06 | 0.11 |
| $(\gamma, \alpha n)$ | — | 58 | 122 | 293 | — | 0.04 | 0.05 | 0.13 |
| **All 3-prong stars this includes:** | — | 522 | 601 | 1345 | — | 0.41 | 0.23 | 0.62 |
| $(\gamma, p\alpha)$ | — | 162 | 202 | 869 | — | 0.13 | 0.08 | 0.40 |
| $(\gamma, p\alpha n)$ | — | 82 | 46 | 87 | — | 0.06 | 0.02 | 0.04 |
| $(\gamma, 2p)$ | — | 103 | 212 | 172 | — | 0.08 | 0.08 | 0.08 |
| $(\gamma, 2pn)$ | 63 | 82 | 102 | 59 | 0.02 | 0.06 | 0.04 | 0.03 |
| $(\gamma, 2\alpha)$ | — | 37 | — | 142 | — | 0.03 | 0.004 | 0.06 |
| $(\gamma, 2\alpha n)$ | — | 44 | — | 16 | — | 0.03 | 0.002 | 0.007 |
| **All 4-prong stars this includes:** | — | 721 | 208 | 162 | — | 0.56 | 0.08 | 0.07 |
| $(\gamma, 3\alpha pn)$ | — | 618 | — | — | — | 0.48 | — | — |
| $(\gamma, 4\alpha)$ | — | — | 82 | — | — | — | 0.03 | — |
| **All 5-prong stars this includes:** | — | 65 | 97 | 47 | — | 0.05 | 0.04 | 0.02 |
| $(\gamma, 2p2n3\alpha)$ | — | — | 76 | — | — | — | 0.03 | — |
| $(\gamma, 3p3n2\alpha)$ | — | 38 | — | — | — | 0.03 | — | — |
| **6-prong stars** | — | — | 10 | 29 | — | — | 0.004 | 0.01 |
| **7-prong stars** | — | 1 | — | 2 | — | 0.001 | — | 0.001 |

different observers. Below we give results of the scanning of 5300 pictures on nitrogen, 8500 pictures on oxygen, and 8500 pictures on neon.

## 4. EXPERIMENTAL RESULTS

The numbers of the different photonuclear reactions observed in nitrogen, oxygen, and neon are given in Table II together with their yield relative to the $(\gamma, p)$ reaction for each element. The absolute value of the yield of the reactions

$$Y = \int_0^{170} \sigma(E)\,\eta(E)\,dE$$

is given in Table III. For comparison, the corresponding data for helium are also given in Tables II and III.[10]

One sees from Table II that the yield ratio of the reactions $(\gamma, pn)$ and $(\gamma, p)$ in the "α-particle" nuclei $O^{16}$ and $Ne^{20}$ are approximately equal and have the value ~ 20%. This agrees approximately with the yield ratio of the reaction $(\gamma, pn)$ and $(\gamma, p)$ in free α particles, where it is 0.17. For $N^{14}$ the yield ratio of $(\gamma, pn)$ and $(\gamma, p)$ turned out to be much larger, namely 1.90 ± 0.07.* Thus the reaction $(\gamma, pn)$ is the most important photonuclear reaction in nitrogen in spite of having a higher threshold than the $(\gamma, p)$ and $(\gamma, n)$ reactions.

*The yield ratio of the reactions $(\gamma, pn)$ and $(\gamma, p)$ in nitrogen was reported earlier as 1.49 at $E_{\gamma max} = 200$ MeV[11], 1.65 ± 0.35 at $E_{\gamma max} = 100$ MeV[12], and 1.25 at $E_{\gamma max} = 90$ MeV.[13] These experiments were also performed in a cloud chamber.

The large yield of the reaction $(\gamma, pn)$ and the relatively low yield of the reactions $(\gamma, p)$ and $(\gamma, n)$ in nitrogen can evidently be explained by the low thresholds for emission of the valence nucleons from the nuclei $N^{13}$ and $C^{13}$. Indeed, one can assume that the reaction $(\gamma, pn)$ in nitrogen proceeds as the result of the following processes:

1) $N^{14}(\gamma, n)N^{13*}$, $N^{13*} \rightarrow C^{12} + p$ (reaction threshold 1.94MeV);
2) $N^{14}(\gamma, p)C^{13*}$, $C^{13*} \rightarrow C^{12} + n$ (reaction threshold 4.95MeV);
3) $N^{14}(\gamma, pn)C^{12}$.

The first two reactions are single-particle transitions; the third can be due to the quasideuteron process. The reaction (1) is already possible if the nucleus $N^{13*}$ is left in the first excited state which has an energy (3.51 MeV) which is above the threshold for emission of protons from $N^{13}$. The reaction (2) is possible if the nucleus $C^{13*}$ is left with an excitation energy above 5 MeV. One thus would think that the reaction $N^{14}(\gamma, n)N^{13}$ can be observed only in ground state transitions. All transitions going to excited states of $N^{13}$ should lead to the reaction $(\gamma, pn)$. Similarly, the reaction $N^{14}(\gamma, p)C^{13}$ is associated with transitions in which the nucleus $C^{13}$ is left in the ground state or the first odd excited state. The transitions in which the nucleus $C^{13}$ is left in a higher excited state also lead to the reaction $(\gamma, pn)$. One notes also the following features in Tables II and III:

A. The yield of four prong stars in nitrogen [reaction $(\gamma, pn3\alpha)$] is 3.5 times larger than the

**Table III**

| Reaction type | Absolute values of the photonuclear yields, Y, mb | | | |
|---|---|---|---|---|
| | $He^4$ | $N^{14}$ | $O^{16}$ | Ne |
| $(\gamma, p)$ | 1.18 | 3.08 | 6.13 | 7.47 |
| $(\gamma, n)$ | 1.12 | 1.71 | 3.67 | 3.80 |
| $(\gamma, pn)$ | 0.20 | 5.83 | 1.32 | 1.47 |
| $(\gamma, \alpha)$ | | 0.39 | 0.36 | 0.83 |
| $(\gamma, \alpha n)$ | | 0.14 | 0.29 | 1.00 |
| **All 3-prong stars this includes:** | | 1.26 | 1.41 | 4.60 |
| $(\gamma, p\alpha)$ | | 0.39 | 0.48 | 2.97 |
| $(\gamma, p\alpha n)$ | | 0.20 | 0.11 | 0.30 |
| $(\gamma, 2p)$ | | 0.25 | 0.50 | 0.59 |
| $(\gamma, 2pn)$ | 0.026 | 0.20 | 0.24 | 0.20 |
| $(\gamma, 2\alpha)$ | | 0.09 | | 0.49 |
| $(\gamma, 2\alpha n)$ | | | | 0.05 |
| **All 4-prong stars this includes:** | | 1.74 | 0.49 | 0.55 |
| $(\gamma, 3\alpha pn)$ | | 1.49 | | |
| $(\gamma, 4\alpha)$ | | | 0.19 | |
| **All 5-prong stars this includes:** | | 0.19 | 0.23 | 0.16 |
| $(\gamma, 2p2n3\alpha)$ | | | 0.18 | |
| **6-prong stars** | | | 0.02 | 0.10 |
| **7-prong stars** | | | | 0.001 |

yield of four prong stars in oxygen and neon. A reaction of this type obviously comes about in the decay of a highly excited $C^{12}$ nucleus from a $(\gamma, pn)$ reaction (excitation energy larger than $\sim 7.3$ MeV).

B. The yield of three prong stars in neon is high. The main part of these is connected with the reaction $(\gamma, p\alpha)$.* Evidently the reaction $Ne^{20}(\gamma, p\alpha)N^{15}$ is due to emission of an $\alpha$-particle from an excited state of $F^{19}$ produced in a $(\gamma, p)$ reaction.

C. The small $(\gamma, \alpha)$ yield in all investigated nuclei.

## 5. DISCUSSION OF THE RESULTS

Using the absolute yields of the different reactions in the nuclei $N^{14}$, $O^{16}$, and Ne given in Table III, we have evaluated the integrated cross sections of the reactions. To that end the yield of the reactions is written in the form

$$Y = \int_0^{170} \sigma(E)\,\eta(E)\,dE = \overline{\eta(E)}\,\sigma_0 = \eta(\widetilde{E})\,\sigma_0,$$

$$\sigma_0 = \int_0^{170} \sigma(E)\,dE,$$

where $\sigma_0$ is the integrated cross section of the reaction and $\eta(\widetilde{E})$ is the intensity of the bremsstrahlung spectrum at some mean energy $\widetilde{E}$. From this we have

$$\sigma_0 = Y/\eta(\widetilde{E}).$$

*Similar results have been obtained by Komar and Yavor.[14]

If the cross sections were $\delta$-functions the value $\widetilde{E}$ would coincide with the resonance energy. Since in actuality the absorption cross sections differ from zero appreciably even at excitation energies exceeding $E_{res}$ considerably, $\widetilde{E} > E_{res}$. We assume for our evaluations $\widetilde{E} = 2\epsilon$, where $\epsilon$ is the threshold of the particular reaction. The basis for this choice of $\widetilde{E}$ is the evaluation of $\widetilde{E}$ for reactions for which the integrated cross section has been determined directly from the effective cross section. For example, according to Spiridonov and Gorbunov[10,15] in the case of helium $\widetilde{E} = 35$ MeV for the reactions $(\gamma, p)$ and $(\gamma, n)$ while the threshold is $\epsilon \approx 20$ MeV; for the reaction $(\gamma, pn)$, $\widetilde{E} = 58$ MeV and $\epsilon = 26$ MeV; for carbon we find from the data of Barber et al[8] $\widetilde{E} = 35$ MeV and $\epsilon = 18.7$ MeV for the reaction $C^{12}(\gamma, n)C^{11}$.

Adding the values of $\sigma_0$ for the different reactions we obtain the integrated photon absorption cross section for the nucleus under investigation. A similar procedure was used to evaluate $\sigma_{-1}$ and $\sigma_{-2}$. It should be mentioned that in such an evaluation $\sigma_{-1}$ is determined much better than either $\sigma_0$ or $\sigma_{-2}$ since the bremsstrahlung spectrum differs only little from $1/E$. The quantities $\sigma_0$, $\sigma_{-1}$, and $\sigma_{-2}$ for the different reactions and also for the photon absorption cross sections of the nuclei $N^{14}$, $O^{16}$, and Ne are given in Table IV. At the bottom of Table IV are given the theoretical values of the cross sections $\sigma_0$, $\sigma_{-1}$, $\sigma_{-2}$ and also the ratio of the experimental and theoretical values.

The theoretical value of the integrated cross section for electric dipole absorption can be evaluated by means of the sum rule[5]

**Table IV**

| Reaction type | $\sigma_0$, MeV-mb | | | | $\sigma_{-1}$, mb | | | | $\sigma_{-2}$, mb-MeV$^{-1}$ | | | |
|---|---|---|---|---|---|---|---|---|---|---|---|---|
| | $He^4$ | $N^{14}$ | $O^{16}$ | Ne | $He^4$ | $N^{14}$ | $O^{16}$ | Ne | $He^4$ | $N^{14}$ | $O^{16}$ | Ne |
| $(\gamma, p)$ | 38 | 38 | 129 | 165 | 1.09 | 2.5 | 5.3 | 6.5 | 0.035 | 0.14 | 0.22 | 0.25 |
| $(\gamma, n)$ | 44 | 31 | 105 | 115 | 1.09 | 1.5 | 3.4 | 3.5 | 0.031 | 0.06 | 0.11 | 0.10 |
| $(\gamma, pn)$ | 12 | 128 | 59 | 66 | 0.18 | 5.1 | 1.3 | 1.4 | 0.003 | 0.18 | 0.03 | 0.03 |
| $(\gamma, \alpha)$ | — | 8 | 4 | 6 | — | 0.3 | 0.3 | 0.6 | — | 0.01 | 0.02 | 0.07 |
| $(\gamma, \alpha n)$ | — | 5 | 15 | 38 | — | 0.1 | 0.3 | 1.0 | — | 0.003 | 0.005 | 0.02 |
| Stars: | | | | | | | | | | | | |
| 3-prong | — | 53 | 71 | 151 | — | 1.2 | 1.4 | 4.2 | — | 0.03 | 0.03 | 0.12 |
| 4-prong | — | 70 | 27 | 34 | — | 1.6 | 0.5 | 0.5 | — | 0.04 | 0.01 | 0.01 |
| 5-prong | — | 14 | 23 | 15 | — | 0.2 | 0.3 | 0.2 | — | 0.002 | 0.003 | 0.003 |
| 6-prong | — | — | 5 | 10 | — | — | 0.03 | 0.1 | — | — | 0.001 | 0.001 |
| $\sigma_{exp}$* | 95±7 | 347 | 438 | 600 | 2.40±0.15 | 12.5 | 12.8 | 18.0 | 0.07±0.005 | 0.46 | 0.43 | 0.60 |
| $\sigma_{theor}$** | 60 | 210 | 240 | 300 | 2.3 | 12.1 | 13.1 | 19.5 | 0.023 | 0.18 | 0.23 | 0.33 |
| $\sigma_{exp}/\sigma_{theor}$ | 1.6 | 1.65 | 1.8 | 2.0 | 1.04 | 1.03 | 0.98 | 0.9 | 3.0 | 2.6 | 1.8 | 1.8 |

* $\sigma_{exp}$—experimental value of the integrated absorption cross sections $\sigma_0$, $\sigma_{-1}$ and $\sigma_{-2}$.
** The theoretical values $\sigma_{theor}$ have been calculated by means of the expressions: $\sigma_0 = 60(NZ/A)$ MeV-mb; $\sigma_{-1} = 0.36\,A^{4/3}$ mb; $\sigma_{-2} = 2.25\,A^{5/3}$ $\mu$b-MeV$^{-1}$.

$$\sigma_0 = \int \sigma dE = -\frac{2\pi^2}{\hbar c}\left\{\left[[H, d_z], d_z\right]\right\}_{00},$$

where H is the nuclear Hamiltonian and $d_z = \Sigma e_i z_i$ is the electric dipole operator (the z axis has been chosen in the direction of the photon polarization).

The result of the evaluation of $\sigma_0$ depends strongly on the form of the potential. In particular, a calculation with a velocity-independent shell-model potential leads to

$$(\sigma_0)_{TRK} = \frac{2\pi^2 e^2 \hbar}{Mc}\frac{NZ}{A} = 0{,}060\,\frac{NZ}{A}\,\text{MeV}\cdot\text{b}$$

(the Thomas-Reiche-Kuhn sum rule, see e.g., [16]). If one introduces two-body exchange forces or velocity-dependent shell-model potentials, the integrated cross section is increased considerably. Levinger and Bethe[5] have shown that in this case the integrated cross section can be satisfactorily approximated by the expression

$$\sigma_0 = 0.060\,\frac{NZ}{A}(1+\Delta)\,\text{MeV}\cdot\text{b}$$

where $\Delta$ is the contribution of the exchange forces. They have found that for different assumptions on the form and the parameters of the potential $\Delta \approx 0.4$ if the share of the exchange forces $X = 0.5$. Rand[17] has obtained a value $\Delta = 0.9$ for a shell model with a velocity dependent potential.[18]

In Table IV we have used $(\sigma_0)_{TRK}$ for the theoretical values. It coincides with the value obtained by Goldhaber and Teller[19] for the classical collective model. One sees from Table IV that the experimental values of the integrated cross section for the nuclei $N^{14}$, $O^{16}$, and Ne are 1.6 to 2 times larger than $(\sigma_0)_{TRK}$. Thus the experimentally determined contribution of the exchange forces to the integrated cross section ($\Delta = 0.6$ to 1.0) lies within the range of the theoretical values of Levinger and Bethe[5] and of Rand.[17] The experimental value obtained for helium directly from the effective cross section[10] is 1.6 times $(\sigma_0)_{TRK}$ ($\Delta = 0.6$). It agrees well with the results of calculations[20] in which a mixture of exchange forces of the Rosenfeld or Inglis type is used.

As noted above, a certain arbitrariness is associated with the choice of $\tilde{E}$. In any case it can be affirmed that $1.5\epsilon < \tilde{E} \leq 2\epsilon$ (indeed, for $O^{16}$ and $Ne^{20}$ the energy $1.5\epsilon$ for the reaction $(\gamma, n)$ corresponds to the peak of the giant resonance, while for the $(\gamma, p)$ reaction it is below $E_{res}$). Any value of $\tilde{E}$ within this interval used for the evaluation of the integrated cross sections will yield an experimental value not lower than $1.4\,(\sigma_0)_{TRK}$.

A direct measurement of the integrated photon absorption cross sections in light nuclei exists only for deuterium[21] and helium.[22] For medium and heavy nuclei the integrated absorption cross sections are obtained from measurements of total neutron yields.[23-25] In the majority of cases the results apply only up to an excitation energy of 30 MeV. For example, Nathans and Halpern[25] determined the integrated cross sections for a number of medium and heavy nuclei at $E_{\gamma\,max} = 24$ MeV. The results lie between $(\sigma_0)_{TRK}$ and $1.9\,(\sigma_0)_{TRK}$ ($\Delta = 0$ to 0.9).

An increase of the upper limit of the integration can lead to a large increase in $\sigma_0$. For example, Jones and Terwilliger[26] obtained for tantalum $\sigma_0$ ($\leq 150$ MeV) = 6 MeV-b and $\sigma_0$ ($\leq 25$ MeV) = 4 MeV-b while for tantalum $(\sigma_0)_{TRK}$ = 2.6 MeV-b.

Considering the rather large uncertainties associated both with the theoretical and the experimental evaluations of the integrated cross section, we conclude that there exists satisfactory agreement between the experimental values of the integrated photon absorption cross sections of $N^{14}$, $O^{16}$, and Ne and the values calculated for the electric dipole absorption with account of the exchange forces. This indicates that the electric dipole transitions play the predominant role in the photon absorption by light nuclei.

One sees further from Table IV that the reactions leading to the emission of a single nucleon make a relatively small contribution to the integrated absorption cross section (20% in $N^{14}$, 50% in $O^{16}$, and 45% in Ne). Evidently this result will be difficult to reconcile with a theory of the nuclear photoeffect based on a shell model in which nucleon correlations are not taken into account.

Finally, Table IV shows that the integrated cross sections for the reactions $(\gamma, p)$ and $(\gamma, n)$ differ but little in all investigated nuclei and that the cross sections for the reaction $(\gamma, \alpha)$ are very small. As has been shown by Gell-Mann and Telegdi,[27] these results are connected with the charge independence of the nuclear forces.

The quantities $\sigma_{-1}$ and $\sigma_{-2}$ are easier to compare with theory than $\sigma_0$. This is due to their independence of the character of the nuclear forces. In contrast to $\sigma_0$ they depend only on the properties of the nuclear ground state. Furthermore, as has already been pointed out the precision with which $\sigma_{-1}$ can be experimentally determined is much higher than that of the determination of $\sigma_0$. The theoretical evaluation of $\sigma_{-1}$ has been performed in a number of papers[5,28-30] on the basis of the independent particle model. Thus it was shown by Levinger and Bethe[5] that for electric dipole absorption $\sigma_{-1}$ depends only on the mean square radius of the nuclear charge distribution if one neglects all effects of nucleon-nucleon correlations.

The effect of the nonuniformity of the particle distribution due to the Pauli principle and also the influence of the Coulomb forces was investigated by Khokhlov.[28] He used the independent particle model with a finite square well and found for $\sigma_{-1}$ the expression

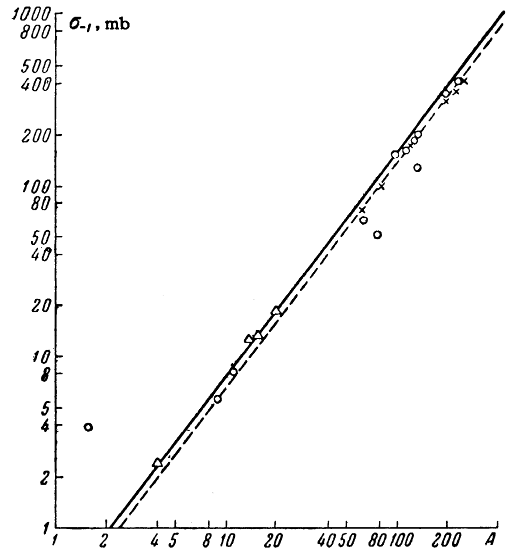


FIG. 2. Dependence of $\sigma_{-1}$ on A. Crosses and dashed line: results of the calculation of Khokhlov[28] and Levinger and Kent[29] using a finite square well with $r_0 = 1.2 \times 10^{-13}$ cm; circles: results of the analysis of experimental data by Khokhlov[28] and Levinger [32]; triangles: our data for $N^{14}$, $O^{16}$ and Ne as well as the value of $\sigma_{-1}$ for He.[15] Full line: calculation using a harmonic oscillator shell model.[30]

$$\sigma_{-1} = \frac{4\pi^2}{3}\left(\frac{e^2}{\hbar c}\right)\frac{NZ}{A-1}(1-\Lambda)\overline{R_c^2},$$

where $\overline{R_c^2}$ is the mean square radius of the nuclear charge distribution and the quantity $\Lambda = 0.84 \times (1 + 22/A)^{-1}$ describes the Pauli-correlations of the particles.

Foldy[30] has shown that one has to correct this formula for the finite charge distribution of the proton if the proton is not polarized to any great extent when placed in close vicinity of other nucleons. This correction leads to the following expression:

$$\sigma_{-1} = \frac{4\pi^2}{3}\left(\frac{e^2}{\hbar c}\right)\frac{NZ}{A-1}(1-\Lambda)\left(\overline{R_c^2}-\overline{R_p^2}\right).$$

Levinger[32] and Khokhlov[28] have analyzed the available experimental material concerning the measurements of $\sigma_{-1}$. In Fig. 2 we have reproduced Levinger's graph, which contains the data evaluated by Khokhlov and Levinger. In the same graph we have plotted our experimenta results of $\sigma_{-1}$ for $N^{14}$, $O^{16}$, and Ne as well as the value of $\sigma_{-1}$ for $He^4$ from [10]. One sees that our experimental points agree well with the theoretical curve $\sigma_{-1} = 0.36\,A^{4/3}$ mb which has been obtained[30] from a harmonic oscillator model.

Thus the experimental results agree well with the theoretical evaluations based on the independent particle model not only for medium and heavy nuclei but also for light ones. As has been shown

Table V. Parameters of the charge distribution in the nuclei $He^4$, $N^{14}$, $O^{16}$, $Ne^{20}$

| Nucleus | $He^4$ | $N^{14}$ | $O^{16}$ | $Ne^{20}$ |
|---|---|---|---|---|
| $R_c \times 10^{13}$ cm | 1,57±0.06 | 2.40 | 2.33 | 2,56 |
| $R \times 10^{13}$ cm* | 2.03±0,08 | 3.10 | 3.00 | 3,30 |
| $r_0 \times 10^{13}$ cm | 1.28±0.05 | 1.29 | 1.19 | 1.22 |
| $r_c$ from[34] | 1.61±0.03 | — | 2,64 | — |

*R is the radius of the nucleus assuming uniform charge distribution.

by Okamoto,[33] the dynamical correlations between nucleons have a small influence on the value of $\sigma_{-1}$.

In Table V we list the mean square radii $R_c$ of the charge distributions and the values $r_0 = R/A^{1/3}$ obtained from the experimental values of $\sigma_{-1}$ for $N^{14}$, $O^{16}$, and Ne using Khokhlov's formula with Foldy's correction. For comparison we have also listed the values for $He^4$[15] and the results from high-energy electron scattering experiments.[34] One sees from Table V that the results obtained for the radius of the charge distribution from the nuclear photoeffect agree well with the results obtained from high energy electron scattering experiments.

Finally, we compare our experimental values $\sigma_{-2}$ for $N^{14}$, $O^{16}$, and Ne with the theoretical values computed by Migdal.[35] From a semiclassical treatment of the nuclear polarizability, which considers the protons and neutrons as interpenetrating liquids, he evaluated the dipole moment induced in the nucleus by a static electric field. He showed that the polarizability equals.

$$\alpha = \frac{e^2R^2A}{40K} = \frac{\hbar c}{2\pi^2}\int\frac{\sigma(E)}{E^2}\,dE,$$

where K is the symmetry energy constant is the Weizsäcker semi-empirical formula. From this follows

$$\sigma_{-2} = \frac{\pi^2}{20}\left(\frac{e^2}{\hbar c}\right)\frac{R^2A}{K}.$$

With $R = 1.2\,A^{1/3} \times 10^{-13}$ cm and K = 23 MeV this gives[32]

$$\sigma_{-2} = 2.25A^{5/3}\ \mu b \cdot MeV^{-1}.$$

Levinger analyzed the available experimental data and evaluated the quantity $\sigma_{-2}$ for a number of nuclei.[32] In Fig. 3 we have reproduced his results, with $\sigma_{-2}$ plotted as a function of A. The open circles in the same drawing are our results on $N^{14}$, $O^{16}$, and Ne as well as on He.[22] One sees from Table IV and Fig. 3 that the experimental values of $\sigma_{-2}$ exceed for these nuclei considerably the theoretical value $\sigma_{-2} = 2.25\,A^{5/3}\ \mu b$ $MeV^{-1}$ (dotted line in Fig. 3). They fit, however,

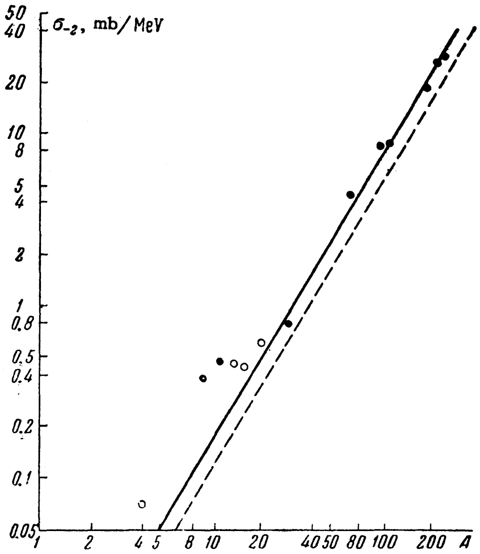


FIG. 3. Dependence of $\sigma_{-2}$ on A. Full circles: results obtained by Levinger [32] from the analysis of experimental data; open circles: our data for $N^{14}$, $O^{16}$, and Ne as well as the value of $\sigma_{-2}$ for He. [22]

satisfactorily the expression $\sigma_{-2} = 3.5\,A^{5/3}\ \mu b$ $MeV^{-1}$ (full line in Fig. 3), which according to Levinger describes well the experimental results on medium and heavy nuclei. The experimental value of $\sigma_{-2}$ differs much more from the theoretical value for nitrogen than for oxygen and neon. This possibly indicates that the polarizability of non-closed shell nuclei is larger than that of nuclei with closed shells.

## 6. CONCLUSIONS

In the present work the absolute yields of different photonuclear reactions have been measured for nitrogen, oxygen, and neon. Experimental values for $\sigma_0$, $\sigma_{-1}$, and $\sigma_{-2}$ have been determined which can be compared with theoretical sum rule calculations.

The experimental integrated cross sections agree well with the theoretical values for the electric dipole absorption cross section calculated with inclusion of exchange forces. However, it should be pointed out that the experimental results give a somewhat larger contribution of the exchange forces ($\Delta$ = 0.6 to 1.0) than a theory based on the independent particle model (for example, according to Levinger and Bethe[5] $\Delta = 0.4$). Possibly this points to the existence of strong nucleon-nucleon correlations in the nucleus and to the necessity of inclusion of the influence of tensor forces.[36]

The integrated cross sections for the reactions ($\gamma$, p) and ($\gamma$, n) differ little in all investigated nuclei and the cross sections for the reaction

$(\gamma, \alpha)$ are very small. This agrees with the expectations based on the charge independence of the nuclear forces.

The reactions leading to the emission of one particle give a relatively small contribution ($\sim 50\%$ for $O^{16}$ and Ne; $\sim 20\%$ for $N^{14}$) to the integrated absorption cross section.

The moments of the absorption cross section $\sigma_{-1}$ turned out to be in good agreement with the theoretical values calculated on the basis of the independent particle model. The mean square radii of the charge distributions were calculated from the experimental values of $\sigma_{-1}$ for $N^{14}$, $O^{16}$, and Ne.

The quantities $\sigma_{-2}$ exceed considerably Migdal's sum-rule values. They agree well with the dependence of $\sigma_{-2}$ on A determined from experimental values in medium and heavy nuclei.[32]

In contrast to the "$\alpha$-particle" nuclei $O^{16}$ and $Ne^{20}$ and also the free $\alpha$-particle, $N^{14}$ shows an anomalously high $(\gamma, pn)$ yield. The existence of this anomaly confirms the predictions of the shell model concerning the strong dependence of the nuclear photoeffect on the structure of the nucleus.

In conclusion the authors express their gratitude to A. G. Gerasimov who participated in the construction of the apparatus, and also to A. I. Orlova, N. Pluzhnikova, V. A. Sakovich, Yu. A. Fomin, and V. E. Yakushkin for their help in the taking and developing of the cloud chamber pictures.

[1] J. P. Elliott and B. H. Flowers, Proc. Roy. Soc. **A242**, 57 (1957).

[2] Balashov, Shevchenko, and Yudin, Trudy konferentsii po yadernym reaktsiyam pri malykh i srednikh energiyakh (Proceedings of the Conference of Nuclear Reactions at Low and Medium Energies), AN SSSR (1960).

[3] G. Brown and M. Bolsterli, Phys. Rev. Lett. **3**, 472 (1959).

[4] Balashov, Shevchenko, and Yudin, JETP **41**, 1929 (1961), Soviet Phys. JETP **14**, 1371 (1962).

[5] J. S. Levinger and H. A. Bethe, Phys. Rev. **78**, 115 (1950).

[6] Gerasimov, Gorbunov, Dubrovina, Kaipov, Kuvatov, Orlova, Osipova, Sakovich, Silaeva, Fomin, and Cerenkov, Trudy Tashkent-skoĭ konferentsii po mirnomu ispol'zovaniyu atomnoĭ energii 1959 (Proc. of the Tashkent Conference on Peaceful Uses of Atomic Energy 1959), AN UzbSSR (1961).

[7] Gerasimov, Gorbunov, Ivanov, Kutsenko, and Spiridonov, PTÉ **3**, 10 (1957).

[8] Barber, George, and Reagan, Phys. Rev. **98**, 73 (1955).

[9] O'Connell, Dyal, and Goldemberg, Phys. Rev. **116**, 173 (1959).

[10] A. N. Gorbunov and V. M. Spiridonov, JETP **33**, 21 (1957), Soviet Phys. JETP **6**, 16 (1958).

[11] D. Balfour and D. C. Menzies, Proc. Phys. Soc. **75**, 543 (1960).

[12] E. R. Gaerttner and M. L. Yeater, Phys. Rev. **77**, 570 (1950).

[13] Komar, Krzhemenek, and Yavor, DAN SSSR **131**, 283 (1960), Soviet Phys. Doklady **5**, 295 (1960).

[14] A. P. Komar and I. P. Yavor, JETP **32**, 614 (1957), Soviet Phys. JETP **5**, 508 (1957).

[15] A. N. Gorbunov and V. M. Spiridonov, JETP **34**, 862, 866 (1958), Soviet Phys. JETP **7**, 596, 600 (1958).

[16] J. S. Levinger, Nuclear Photodisintegration, Oxford Univ. Press (1960).

[17] S. Rand, Phys. Rev. **107**, 208 (1957).

[18] N. Johnson and E. Teller, Phys. Rev. **98**, 783 (1955).

[19] M. Goldhaber and E. Teller, Phys. Rev. **74**, 1046 (1948).

[20] M. L. Rustgi and J. S. Levinger, Phys. Rev. **106**, 530 (1957).

[21] J. S. Levinger, Phys. Rev. **97**, 970 (1955).

[22] A. N. Gorbunov, Proc. of the P. N. Lebedev Phys. Inst., Acad. Sci. U.S.S.R. **13**, 174 (1960).

[23] E. G. Fuller and M. S. Weiss, Phys. Rev. **112**, 560 (1958).

[24] Montalbetti, Goldemberg, and Katz, Phys. Rev. **91**, 659 (1953).

[25] R. Nathaus and J. Halpern, Phys. Rev. **93**, 437 (1954).

[26] L. W. Jones and K. M. Terwilliger, Phys. Rev. **91**, 699 (1953).

[27] M. Gell-Mann and V. L. Telegdi, Phys. Rev. **91**, 169 (1953).

[28] Yu. K. Khokhlov, DAN SSSR **97**, 239 (1954); JETP **32**, 124 (1957), Soviet Phys. JETP **5**, 88 (1957).

[29] J. S. Levinger and D. C. Kent, Phys. Rev. **95**, 418 (1954).

[30] J. S. Levinger, Phys. Rev. **97**, 122 (1955).

[31] L. L. Foldy, Phys. Rev. **107**, 1303 (1957).

[32] J. S. Levinger, Phys. Rev. **107**, 554 (1957).

[33] K. Okamoto, Phys. Rev. **116**, 428 (1959).

[34] R. Hofstadter, Ann. Rev. Nucl. Sci. **7**, 231 (1957).

[35] A. B. Migdal, JETP **15**, 81 (1945).

[36] K. Okamoto and K. Hasegawa, Preprint.

Translated by M. Danos
120